

Quantum skyrmions and the destruction of long-range antiferromagnetic order in the high- T_c superconductors $\text{La}_{2-x}\text{Sr}_x\text{CuO}_4$ and $\text{YBa}_2\text{Cu}_3\text{O}_{6+x}$

Eduardo C. Marino and Marcello B. Silva Neto

Instituto de Física, Universidade Federal do Rio de Janeiro, Caixa Postal 68528, Rio de Janeiro - RJ, 21945-970, Brazil
(October 28, 2018)

We study the destruction of long range antiferromagnetic order in the high- T_c superconductors $\text{La}_{2-x}\text{Sr}_x\text{CuO}_4$ and $\text{YBa}_2\text{Cu}_3\text{O}_{6+x}$. The CP^1 -nonlinear sigma model formulation of the two-dimensional quantum Heisenberg antiferromagnet is used for describing the pure system. Dopants are introduced as independent fermions with an appropriate dispersion relation determined by the shape of the Fermi surface. Skyrmion topological defects are shown to be introduced by doping and their energy is used as an order parameter for the antiferromagnetic order. We obtain analytic expressions for the skyrmion energy as a function of doping which allow us to plot, without adjustable parameters, the curves $T_N(x_c) \times x_c$ and $M(x) \times x$, for the two compounds, in good quantitative agreement with the experimental data.

PACS number(s): 74.72.Bk, 74.25.Ha

High-temperature superconductivity is by now well established to arise from doping quasi two-dimensional (quasi-2D) Mott-Hubbard antiferromagnetic insulators. The doping process initially produces the destruction of the antiferromagnetic ordering, giving place to a quantum spin-liquid disordered phase [1]. The two best studied examples are $\text{La}_{2-x}\text{Sr}_x\text{CuO}_4$ (LSCO) and $\text{YBa}_2\text{Cu}_3\text{O}_{6+x}$ (YBCO) for which the Néel ordered ground state at $x = 0$ is replaced by a quantum disordered state for $x_c \approx 0.02$ [2] and $x_c \approx 0.41$ [3], respectively, at $T = 0$.

It has long been recognized that the pure compounds are well described in terms of an $S = 1/2$ quantum Heisenberg antiferromagnet (QHAF) on a square lattice. The long wavelength spin fluctuations of the latter, on the other hand, are described by the $O(3)$ quantum nonlinear sigma model (QNL σ M) in two space plus one time dimensions [4,5] whose Lagrangian density is

$$\mathcal{L} = \frac{\rho_s}{2} \left[\frac{1}{c^2} (\partial_\tau \mathbf{n})^2 + (\nabla \mathbf{n})^2 \right], \quad (1)$$

where \mathbf{n} is the order parameter field, subject to the constraint $\mathbf{n}^2 = 1$, and ρ_s and c are respectively the spin-stiffness and spin-wave velocity.

The nonlinear sigma model possesses classical topologically nontrivial solutions called *skyrmions* whose energy is $E_s^{cl} = 4\pi\rho_s$. For fully quantized skyrmions, on the other hand, there is a reduction of the skyrmion energy to half of the above classical value [6]

$$E_s = 2\pi\rho_s. \quad (2)$$

Having in mind that the skyrmion energy is reduced by quantum fluctuations, it is natural to expect it to be further reduced by the extra fluctuations introduced through doping. Furthermore, since in the framework of

the NL σ M the skyrmion energy is proportional to the ground state magnetization we can use it as an order parameter for the quantum phase transition associated to the destruction of the antiferromagnetic state.

In this paper we revisit the continuum model proposed in [7], to describe the doping process in YBCO at $T = 0$, and extend it for including also the case of LSCO. The model predicts the creation of skyrmion topological defects precisely at the dopant's positions, as has been proposed earlier [8] (see also [9]). The formation of such magnetic textures causes a reduction of the ground state magnetization. As a consequence, the skyrmion energy itself is lowered and eventually vanishes at the Néel quantum critical point. By computing quantum defect correlation functions at $T = 0$, we obtain analytical expressions for the skyrmion energy as a function of doping, $E_s(x)$, which allow us to plot the curves $M(x) \times x$, for both LSCO and YBCO, in good quantitative agreement with experiment. Subsequently, introducing finite temperature and interlayer coupling, we obtain the antiferromagnetic part of the phase diagram, namely the curve $T_N(x_c) \times x_c$. As we shall discuss below, our analysis is compatible with a picture in which the formation of stripes would occur in LSCO but not in YBCO.

The doping process: The chemical modification of parent compounds of the high- T_c materials here considered produces the introduction of holes in the Oxygen orbitals in the layered CuO_2 planes. In what follows, we shall determine how the skyrmion energy is modified from (2) due to the presence of such holes. We propose that the doped system can be described in terms of a bulk ($T = 0$) $O(3)$ QNL σ M coupled to four-component fermion fields with dispersion relation determined by the shape of the Fermi surface. These represent the holes doped into the in-plane O^{2-} p -orbitals, whereas the nonlinear sigma

field represents the spin density of the active electrons of the Cu^{++} ions. For describing the coupling of the dopants to the Cu^{++} spins, it will be convenient to make use of the CP^1 language, where $\mathbf{n} = z_i^\dagger \vec{\sigma}_{ij} z_j$, with $\vec{\sigma}_{ij}$ being the Pauli matrices and z_i , $i = 1, 2$, complex scalar fields. Then, following [7] (see also [10]), we minimally couple the fermions to the CP^1 fields. This is also consistent with previous results where a minimal coupling of fermions to CP^1 fields was obtained in the long wavelength regime of the spin-fermion model [11]. Let us consider the cases of YBCO and LSCO separately.

a) For YBCO we have an almost circular shape for the Fermi surface, which is centered at $\mathbf{k} = 0$ [12], see Fig. 1a. We can then use the dispersion relation $\epsilon(k) = \sqrt{k^2 v_F^2 + (m^* v_F^2)^2}$, with m^* and v_F being respectively the effective mass and Fermi velocity of the dopants. Observe that close to the Fermi level of the doped system ($\epsilon_F > m^* v_F^2$) the above dispersion relation behaves as $\epsilon(k) - \epsilon_F \simeq v_F(k - k_F)$ as expected. This dispersion relation corresponds to a Dirac kinetic term for the fermions and the doped system can then be described by the partition function

$$\begin{aligned} \mathcal{Z} = & \int \mathcal{D}[\bar{z}, z, \mathcal{A}_\mu, \bar{\psi}, \psi] \delta[\bar{z}z - 1] \delta[j^\mu - \Delta^\mu] \\ & \times \exp \left\{ \int_0^\infty d\tau \int d^2\mathbf{x} \left[2\rho_s (D_\mu z_i)^\dagger (D^\mu z_i) \right. \right. \\ & \left. \left. + \bar{\psi} (i\partial - \frac{m^* v_F}{\hbar} - \gamma^\mu \mathcal{A}_\mu) \psi + \mathcal{L}_H \right] \right\} \end{aligned} \quad (3)$$

where we allow for a residual Hopf term $\mathcal{L}_H = (\theta/2)\epsilon^{\mu\alpha\beta} \mathcal{A}_\mu \partial_\alpha \mathcal{A}_\beta$, which has been shown to exist in the presence of topological defects on the ground state [13]. As usual, $D_\mu = \partial_\mu + i\mathcal{A}_\mu$, with $\partial_\mu = (\partial_\tau/c, \nabla)$, and $\mathcal{A}_\mu = iz_i^\dagger \partial_\mu z_i$ is the Hubbard-Stratonovich CP^1 vector field.

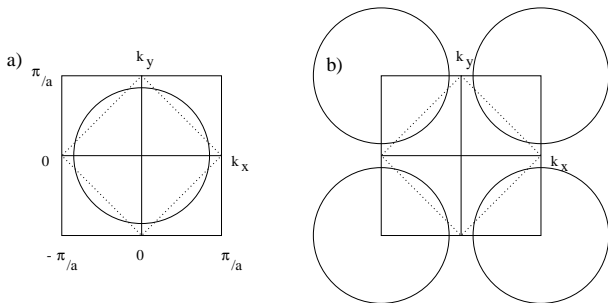


FIG. 1. Approximate Fermi surfaces for: a) $\text{YBa}_2\text{Cu}_3\text{O}_{6+x}$ and b) $\text{La}_{2-x}\text{Sr}_x\text{CuO}_4$ [12].

The second delta functional constraint in (3) is used in order to introduce the in-plane hole concentration parameter δ . In its argument, $j^\mu = \bar{\psi}\gamma^\mu\psi$ and $\Delta^\mu = 4\delta \int_{X,L}^\infty d\xi^\mu \delta^3(z - \xi)$ for a dopant introduced at the position X and moving along the line L . The factor of four in the definition of Δ^μ accounts for the degeneracy of

the adopted representation (4-component) for the Fermi fields. The zeroth component of the associated Lagrange multiplier will be the chemical potential.

It has been shown in [7], that upon integration over the fields $\bar{z}, z, \bar{\psi}, \psi$, the resulting equation of motion for \mathcal{A}_0 is such that a skyrmion topological defect configuration coincides with the dopant position at any time and $\pi\theta = 2\delta$. In other words, holes dress with skyrmions and we see that indeed a Hopf term is required in (3) for nonzero doping. We stress that, because of the CP^1 constraint, a mass term is generated for the \mathcal{A}_μ field. Therefore, as a consequence of screening, there will be neither statistical transmutation nor the generation of spurious in-plane magnetic fields which would be inconsistent with muon spin relaxation experiments [14].

The parameter δ counts the number of holes in the CuO_2 planes. This must be connected to the oxygen stoichiometry parameter x . For YBCO, it is known that the out of plane O-Cu-O chains play an important role in the process of doping. At low doping, $x \leq 0.18$, most of the holes go to the out of plane chains and the system can be considered as pure. In view of this we propose that the density of in-plane charge carriers is related to the oxygen stoichiometry by $\delta = x - 0.18$.

For evaluating the skyrmion energy E_s , we use the fact that skyrmions are topological defects whose quantum properties can be fully described by disorder field operators μ [15,6]. Using these, we are able to calculate the large distance behavior of the skyrmion correlation function, $\langle \mu^\dagger(X)\mu(Y) \rangle \rightarrow e^{-(E_s/\hbar c)|X-Y|/|X-Y|^\nu}$, from which we can extract the skyrmion energy E_s [6]. For the pure system we have that E_s is given by (2). For the partition function (3), we obtain, after integration over \bar{z}, z , and $\bar{\psi}, \psi$ fields, [7]

$$E_s(\delta) = 2\pi\rho_s \left(1 - \frac{\gamma\hbar c}{\pi a_D \rho_s} \delta^2 \right), \quad (4)$$

where $\gamma = \frac{32\pi(9\pi^2-16)}{(\pi^2+16)^2} = 10.9398$ is a numerical factor that comes from the integration over the fermions, and $a_D \equiv a/\sqrt{2} = 2.68 \text{ \AA}$, the minimal distance between two oxygen atoms, is the lattice spacing for dopants. The above skyrmion energy can be put in the form $E_s = 2\pi\rho_s(\delta)$ if we define an effective δ dependent spin-stiffness

$$\rho_s(\delta) = \rho_s \left(1 - \frac{\gamma\hbar c}{\pi a_D \rho_s} \delta^2 \right). \quad (5)$$

We then conclude, after comparing (4) with (2), that the doped system can be described by a QNL σ M with a generalized δ dependent spin-stiffness given by (5).

We can immediately obtain the reduced sublattice magnetization as a function of doping as: $M(x)/M(0) = \sqrt{\rho_s(x)/\rho_s}$. This is plotted in Fig. 2 for $\hbar c = 1.00 \pm 0.05 \text{ eV \AA}$ and $\rho_s = 0.069 \text{ eV}$ [12]. We see that our theoretical prediction is in good agreement with experiment and $\rho_s(\delta)$ vanishes for

$$\delta_c = \sqrt{\frac{\pi\rho_s a_D}{\gamma\hbar c}}. \quad (6)$$

Using the above experimental input, we obtain $\delta_c = 0.23 \pm 0.03$ or $x_c = 0.41 \pm 0.03$ for the quantum critical point.

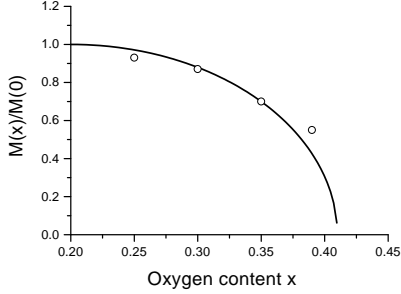


FIG. 2. Reduced sublattice magnetization for $\text{YBa}_2\text{Cu}_3\text{O}_{6+x}$. Experimental data from [16].

b) For the case of LSCO, the Fermi surface is given approximately by the one of Fig. 1b, which has also been observed in ARPES [17]. We shall use the fact that the Fermi surface of LSCO can be obtained by shifting the one of YBCO towards $Q = (\pi/a, \pi/a)$ and symmetry related points in the Brillouin zone. This leads to the new dispersion relation $\epsilon(k) = \sqrt{[(k_x \pm \pi/a)^2 + (k_y \pm \pi/a)^2]v_F^2 + (m^*v_F^2)^2}$, which corresponds to a kinetic term for the fermions in (3) modified by a shifted derivative term. Even though the partition function remains unchanged, this shift will have a non-trivial effect on the skyrmion correlation function and energy because of the constraint on the fermionic density of states. The computation of the skyrmion correlation function proceeds as before [7,6] and we now obtain the following expression for the skyrmion energy

$$E_s(\delta) = 2\pi\rho_s \left(1 - \frac{\gamma\hbar c}{\pi a_D \rho_s} (4\delta)^2 - \frac{2\sqrt{2}\hbar c}{a\rho_s} (4\delta) \right). \quad (7)$$

There are two important differences between (7) and (4). The first one is a linear δ dependence in (7) which is absent in (4). This was generated by the shift in the dispersion relation and is a consequence of the fact that the Fermi surface of LSCO is not centered at $\mathbf{k} = 0$ in the Brillouin zone. The second one is an extra factor of four multiplying δ in (7), which is needed to account for the four branches of the Fermi surface of this compound.

The above skyrmion energy suggests, in accordance to what has been done for the case of YBCO, that the doped system could presumably be described by a QNL σ M with stiffness

$$\rho_s(\delta) = \rho_s \left(1 - \frac{\gamma\hbar c}{\pi a_D \rho_s} (4\delta)^2 - \frac{2\sqrt{2}\hbar c}{a\rho_s} (4\delta) \right). \quad (8)$$

However, the magnetization that would follow from this, according to the same procedure adopted for the case of YBCO, has a faster decrease with doping than the one observed experimentally, as we can infer from the solid line in from Fig. 3. This can be interpreted as a sign of stripes formation in LSCO [18]. Following [19], we observe that the presence of stripes produces an anisotropy which allows us to write $\rho'_s(\delta) = \sqrt{\rho_s^x(\delta)\rho_s^y(\delta)}$, where $\rho_s^x(\delta) \neq \rho_s^y(\delta)$. Assuming that in LSCO stripes are parallel to the y -axis, as the experimental results in [20] suggest, we propose that only the x -component of the spin-stiffness would be affected by doping, implying that $\rho_s^y = \rho_s$ and that $\rho_s^x(\delta)$ is given by (8). The resulting NL σ M has an effective spin-stiffness

$$\rho'_s(\delta) = \rho_s \sqrt{1 - \frac{\gamma\hbar c}{\pi a_D \rho_s} (4\delta)^2 - \frac{2\sqrt{2}\hbar c}{a\rho_s} (4\delta)}. \quad (9)$$

Now the corresponding sublattice magnetization does agree with the experimental data as can be seen from the dashed line in Fig. 3. Both plots in this figure are obtained by using the experimental input $\hbar c = 0.75 \pm 0.03$ eV \AA and $\rho_s = 0.051$ eV [12]. We have also used the well known fact that for LSCO, $x = \delta$. Interestingly, the location of the quantum critical point is not affected by the formation of stripes. In fact, both $\rho_s(\delta)$ and $\rho'_s(\delta)$ vanish at

$$\delta_c = \frac{1}{4} \frac{\sqrt{(2\sqrt{2}\hbar c/a)^2 + 4\gamma\hbar c\rho_s/\pi a_D} - (2\sqrt{2}\hbar c/a)}{2(\gamma\hbar c/\pi a_D)}. \quad (10)$$

which, for the above experimental input, yields the value $x_c = \delta_c = 0.020 \pm 0.003$ for the quantum critical point. We also remark that using the effective spin-stiffness (9), implied by the stripes picture, the reduced sublattice magnetization $M(x)/M(0) = \sqrt{\rho'_s(x)/\rho_s}$ can be written in the form $M(x)/M(0) = (1 - x/x_c)^{1/4}$, thereby producing a critical exponent of 0.25, which is very close to the value of 0.236, empirically obtained by Borsa *et al.* [2].

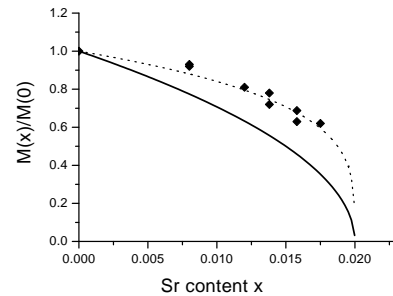


FIG. 3. Reduced sublattice magnetization for $\text{La}_{2-x}\text{Sr}_x\text{CuO}_4$. Experimental data from [2].

The phase diagram: In order to obtain the critical line for the destruction of AF order in the $T \times x$ phase diagram

we must consider a nonzero interlayer coupling J_{\perp} . For this purpose, we shall use the partition function [21]

$$\mathcal{Z} = \int \mathcal{D}\mathbf{n}_i \exp \left\{ -\frac{\rho_s}{2\hbar} \int_0^{\hbar\beta} d\tau \int d^2\mathbf{x} \sum_i \left[\frac{1}{c^2} (\partial_{\tau}\mathbf{n}_i)^2 + (\nabla\mathbf{n}_i)^2 + \alpha(\mathbf{n}_{i+1} - \mathbf{n}_i)^2 \right] \right\} \delta[\mathbf{n}_i^2 - 1], \quad (11)$$

where $\alpha = (1/a^2)J_{\perp}/J_{\parallel}$, with J_{\perp} and J_{\parallel} being respectively the interlayer and intralayer couplings of the underlying microscopic quasi-2D QHAF and $\beta = 1/T$ ($k_B = 1$). Contrary to the strictly 2D case now a finite value for the Néel temperature is obtained to order $1/N$ in a large N expansion [21]:

$$T_N = 4\pi\rho_s \left[\ln \left(\frac{2T_N^2}{\alpha(\hbar c)^2} \right) + 3 \ln \left(\frac{4\pi\rho_s}{T_N} \right) - 0.0660 \right]^{-1}. \quad (12)$$

Now, if we replace in (12) the spin-stiffness ρ_s by our δ dependent expressions (5) and (9), respectively for YBCO and LSCO, and using $J_{\perp}/J_{\parallel} \simeq 5 \times 10^{-5}$, we obtain the phase diagrams plotted in Figs. 4 and 5.

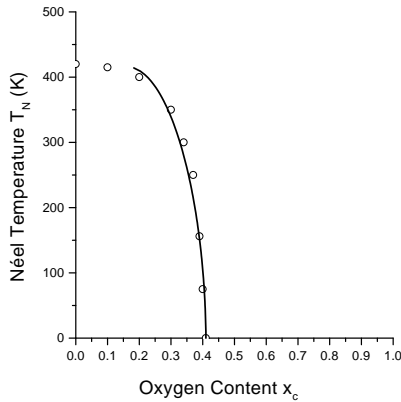


FIG. 4. Antiferromagnetic part of the phase diagram for $\text{YBa}_2\text{Cu}_3\text{O}_{6+x}$. For $x_c < 0.18$, we assume a fixed $T_N = 420\text{K}$. Experimental data from [3].

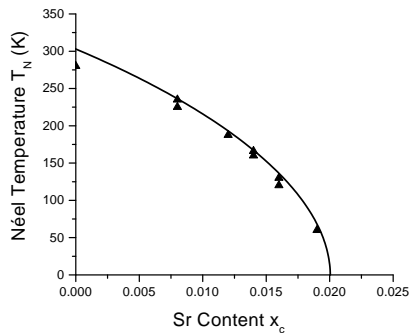


FIG. 5. Antiferromagnetic part of the phase diagram for $\text{La}_{2-x}\text{Sr}_x\text{CuO}_4$. Experimental data from [2].

In summary, our results indicate that the antiferromagnetic phase of the high- T_c cuprates can be correctly described in terms of a generalized NL σ M with an effective, doping dependent, spin-stiffness which carries all the information about the quantum fluctuations introduced by the dopants. This can be inferred from the quantum skyrmion energy which is evaluated after integration over the dopants in a model without adjustable parameters. Also, the results point towards a picture in which charged stripes presumably occur in LSCO, leading to a slower decrease of the sublattice magnetization as a function of doping in comparison to the case where they are absent, see Fig. 3. Apparently, the only effect of such phenomenon is to divide by two the quantum critical exponent of the sublattice magnetization (or the spin-stiffness) without affecting the location of the quantum critical point. Conversely, our results indicate that such phenomenon is absent in YBCO as our model (3) was able to correctly reproduce the zero temperature data for $M(x)/M(0)$, see Fig. 2. This is consistent with density matrix renormalization group calculations in the framework of the n -leg ladder $t - t' - J$ model [22].

As a final comment we would like to remark that for the case of $\text{Bi}_2\text{Sr}_2\text{CaCu}_2\text{O}_{8+x}$ we expect that our result (8) shall correctly reproduce the experimental data without the scaling modifications done for LSCO. Indeed this material, while having a Fermi surface similar to LSCO [23], does not seem to present the formation of stripes.

We are indebted to A. H. Castro Neto, A. A. Katanin, B. Koiller, C. Kübert, E. Miranda and J. Schmalian for many useful comments. We also acknowledge P. Carretta for pointing out Ref. [16]. E.C.M. was partially supported by CNPq and FAPERJ. M.B.S.N was supported by FAPERJ.

-
- [1] P. W. Anderson, *Science* **235**, 1196 (1987).
 - [2] F. Borsa *et al.*, *Phys. Rev. B* **52**, 7334 (1995).
 - [3] J. Rossat-Mignod *et al.*, *Dynamics of Magnetic Fluctuations in High-Temperature Superconductors*, G. Reiter, P. Horsch and G. C. Psaltakis, Eds., Plenum, NY, 1991.
 - [4] F. D. M. Haldane, *Phys. Rev. Lett.* **50**, 1153 (1983).
 - [5] S. Chakravarty, B. I. Halperin and D. R. Nelson, *Phys. Rev. B* **39**, 2344 (1989).
 - [6] E. C. Marino, *Phys. Rev. B* **61**, 1588 (2000)
 - [7] E. C. Marino, *Phys. Lett. A* **263**, 446 (1999).
 - [8] P. B. Wiegmann, *Phys. Rev. Lett.* **60**, 821 (1988); B. I. Schraiman and E. Siggia, *Phys. Rev. Lett.* **61**, 467 (1990).
 - [9] C. Timm and K. H. Bennemann, *Phys. Rev. Lett.* **84**, 4994 (2000).
 - [10] X. G. Wen, *Phys. Rev. B* **39**, 7223 (1989); R. Shankar, *Nucl. Phys. B* **330**, 433 (1990).
 - [11] C. Kübert and A. Muramatsu, *Phys. Rev. B* **47**, 787,

1993.

- [12] A. P. Kampf, Phys. Rep. **249**, 219 (1994).
- [13] F. D. M. Haldane, Phys. Rev. Lett. **61**, 1029 (1988); N. Read and S. Sachdev, Nucl. Phys. B **316**, 609 (1989).
- [14] R. F. Kiefl *et al.*, Phys. Rev. Lett. **64**, 2082 (1990).
- [15] E. C. Marino, in NATO ASI Series, *Applications of Statistical and Field Theory Methods in Condensed Matter*, D. Baeriswyl, A. Bishop and J. Carmelo, Eds., Plenum, NY, (1990).
- [16] C. Bucci *et al.*, Hyperfine Interactions **105**, 71 (1997).
- [17] I. Ano *et al.*, J. Phys. Soc. Jpn. **68**, 1249 (1999).
- [18] P. Carretta *et al.*, cond-mat/9903449.
- [19] A. H. Castro Neto and D. Hone, Phys. Rev. Lett. **76**, 2165 (1995).
- [20] S-W. Cheong *et al.*, Phys. Rev. Lett. **73**, 1003 (1994); E. D. Isaacs *et al.*, Phys. Rev. Lett. **72**, 3421 (1994); T. E. Mason *et al.*, Physica B **199**, 284 (1994).
- [21] V. Yu. Irkhin and A. A. Katanin, Phys. Rev. B **55**, 12318 (1997); Phys. Rev. B **57**, 379 (1998).
- [22] S. R. White and D. J. Scalapino, Phys. Rev. Lett. **80**, 1272 (1998); Phys. Rev. Lett. **81**, 3227 (1998).
- [23] H. Ding *et al.*, Nature **382**, 51 (1996).